Analysis of Vibrational Circular Dichroism Spectra of (*S*)-(+)-2-Butanol by Rotational Strengths Expressed in Local Symmetry Coordinates

Saeko Shin,[†] Munetaka Nakata,[†] and Yoshiaki Hamada*[,‡]

Graduate School of Bio-Applications & Systems Engineering, Tokyo University of Agriculture and Technology, 2-24-16, Naka-cho, Koganei, Tokyo, 184-8588, Japan, and The University of the Air, 2-11, Wakaba, Mihama-ku, Chiba, 261-8586, Japan

Received: August 12, 2005; In Final Form: November 11, 2005

The vibrational circular dichroism (VCD) spectra of (*S*)-(+)-2-butanol have been observed in dilute CS_2 solutions. Two strong VCD bands are assigned mainly to the OH bending modes with the aid of quantum chemical calculations. The calculated VCD spectra corresponding to these bands are shown to depend on the conformation of the OH group. To understand this feature, we have calculated the contribution of each local vibrational mode to the rotational strengths and concluded that the coupling of the group vibrations between the in-plane and out-of-plane modes about the locally assumed symmetry planes play a significant role in VCD. This finding has provided a new scope of VCD in relation to molecular vibrations.

1. Introduction

Vibrational circular dichroism (VCD)[1−3] spectroscopy has become one of the routine methods for investigating chiral molecules. The theoretical understanding of VCD was advanced greatly[4] in the mid 1980s by the magnetic field perturbation theory,[5−7] which is one of the completely analytical methods.[5−11] The density functional theory (DFT)[12] for the calculation of atomic axial tensors (AATs) using gauge-invariant atomic orbitals (GIAOs)[13,14] is available to predict the VCD spectrum accurately. These theoretical calculations supply valuable information about the VCD spectra of chiral molecules, but understanding of the vibrational spectroscopic aspects of VCD still seems to be insufficient. The basic concepts of the normal-mode analysis used in traditional vibrational spectroscopy and structural chemistry are expected to play a valuable role for this purpose.

Certain groups of atoms in a molecule often have their own intrinsic vibrational frequencies. The characteristic frequencies of these groups are influenced by the coupling of two or more group vibrations. This phenomenon provides useful pieces of information about the molecular structure and conformation. One of the convenient ways to analyze vibrational spectra is to evaluate the potential energy distribution (PED),[15] which represents the contribution of a specific vibrational mode expressed in the internal coordinates[16−18] to the normal vibration. The PED is often used to assign the spectrum and analyze the physical meaning of the vibration. However, the applicability of PED for an analysis of VCD spectra has never been discussed to our knowledge.

The VCD bands having large contributions from the OH bending modes of (*S*)-(+)-2-butanol show clear dependence on the conformation. The purpose of the present paper is to introduce a new scope to the understanding of VCD phenomena from the viewpoint of vibrational spectroscopy. We have calculated the contribution of each local vibrational mode to the rotational strengths and explained the above-metioned features of the VCD spectra of (*S*)-(+)-2-butanol in terms of the couplings of vibrational modes.

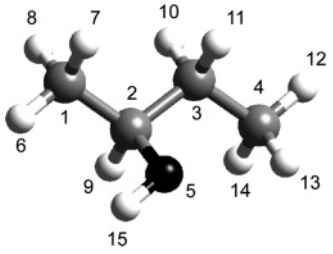

Figure 1. Structure of (*S*)-(+)-2-butanol.

2. Theoretical Calculations and Experiments

Figure 1 shows the molecular structure of (*S*)-(+)-2-butanol. This molecule has four skeletal single bonds, and there may be three stable conformations around the C^2-C^3 and C^2-O bonds. In total, nine rotational isomers are possible. They are named using the two symbols defined in Figure 2. The first capital letters denote the dihedral angle between the C^2-O and C^3-C^4 bonds around the C^2-C^3 bond. The second small letters define the dihedral angle between the O−H and C^2-C^3 bonds around the C^2-O bond. The gauche form is designated as G or g, and the trans form as T or t. The + and − signs represent the anticlockwise and clockwise directions of the dihedral angles, respectively. After geometry optimizations of all nine conformers, we calculated their vibrational frequencies, atom displacements, reduced masses, atomic polar tensors (APTs), and atomic axial tensors (AATs) by using the Gaussian 98 program package[19] at the B3LYP/6-31++G(d,p) level.

The IR and VCD spectra of (*S*)-(+)-2-butanol in CS_2 solution were measured at room temperature. The concentrations of the samples were varied from neat to 0.002 M. The IR and VCD spectra were recorded on a Fourier transform VCD spectrometer, Chiral*ir* (Bomem-BioTools), with a ZnSe PEM and a BaF_2

* Corresponding author. Tel: +81-43-298-4187. Fax: +81-43-298-4379. E-mail: yhamada@u-air.ac.jp.
[†] Tokyo University of Agriculture and Technology.
[‡] The University of the Air.

10.1021/jp0545243 CCC: $33.50
Published on Web 01/20/2006

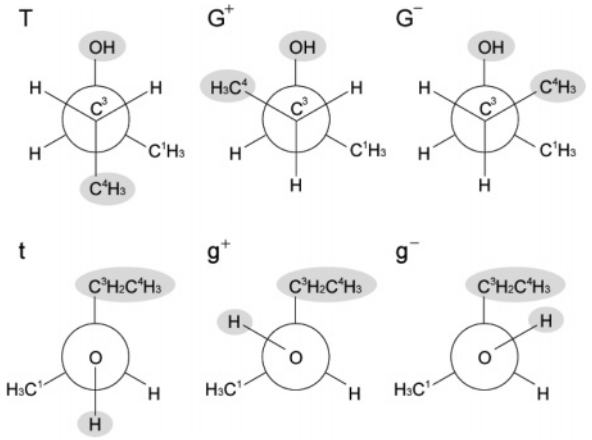

Figure 2. Rotational isomers of (*S*)-(+)-2-butanol.

polarizer. The spectral resolution was fixed to 4 cm^{-1}, and the measurement region was restricted to 2000−800 cm^{-1} using an optical filter transmitting radiations below 2000 cm^{-1}. The spectrum was accumulated on a narrow band MCT detector cooled by liquid N_2. The accumulation times of the VCD spectra were 2 h for the neat and 0.1 M samples, and 4.5 h for the 0.01 M sample, with about 50 scans per minute. The path length of the liquid cell for the VCD measurement was adjusted from 15 μm to 2 mm to obtain a suitable absorbance of about 0.4 to record good VCD signals. BaF_2 was used for the window material. (*S*)-(+)-2-Butanol (purity > 99%) and CS_2 solvent (Aldrich Chemical Co.) were used without further purification.

3. Observed and Calculated Spectra of (*S*)-(+)-2-Butanol

Figure 3a shows the IR spectra of (*S*)-(+)-2-butanol at various concentrations. The bottom trace is the calculated spectrum for all conformers with their relative abundances at room temperature. The frequencies scaled by 0.985 are compared to the observed spectra. The scaling factor was determined empirically to make the calculated 1261 cm^{-1} peak match the observed band at 1242 cm^{-1}.

As is shown in the figure, the neat spectrum differs from the calculated one because of intermolecular hydrogen bonding. Several new peaks appear in the solution spectra; they are enhanced at lower concentrations and shift closer to the calculated ones by dilution. Wang et al. measured the IR and VCD spectra of (*R*)-(−)-2-butanol in solutions[20] and concluded that intermolecular hydrogen bonding persists in 0.029 M CS_2 solution. However, Figure 3a shows that dilute IR spectra, 0.1−0.002 M, are essentially identical. This implies that the molecules in solution below 0.1 M are almost free from the intermolecular hydrogen bonding. This is further supported by our recent measurement of the IR spectrum of this molecule isolated in low-temperature Ar-matrix,[21] where the spectrum is very similar to that in solutions below 0.1 M. Because the spectra below 0.1 M agree with the calculated one, the observed peaks can be assigned by comparison to the calculated spectrum composed of nine conformational isomers.

Figure 3b shows the observed VCD spectra of the CS_2 solutions of (*S*)-(+)-2-butanol. The baselines are corrected by subtracting the averaged spectrum of (*R*) and (*S*) enantiomers. The bottom trace is the calculated VCD spectrum for the (*S*) enantiomers corresponding to the calculated IR spectrum in Figure 3a. Two strong peaks appearing at 1242 and 1072 cm^{-1} in the dilute solutions can be ascribed to the bands of free molecules because they disappear in the neat spectrum.

Figure 4 shows the calculated IR and VCD spectra for (*S*)-(+)-2-butanol. The top trace is constructed from all nine conformers with the relative populations estimated from the ΔG values at 300 K, as listed in Table 1. Judging from the overall agreement between the observed and calculated spectra, the obtained relative populations seem to be reliable. Our results on the populations agree essentially with those calculated at the B3LYP/6-31G(d) level.[20] The two strong VCD bands observed at 1242 and 1072 cm^{-1} in dilute solutions are assigned mainly to the OH bending mode by comparison with the calculated spectrum. This mode is split into two components by mixing with other group modes. The high- and low-frequency bands corresponding to this mode, named "band I and II", respectively, are shaded in Figure 4.

These OH bending bands are classified into three types according to the conformation of the OH group; g^-, g^+, and t.

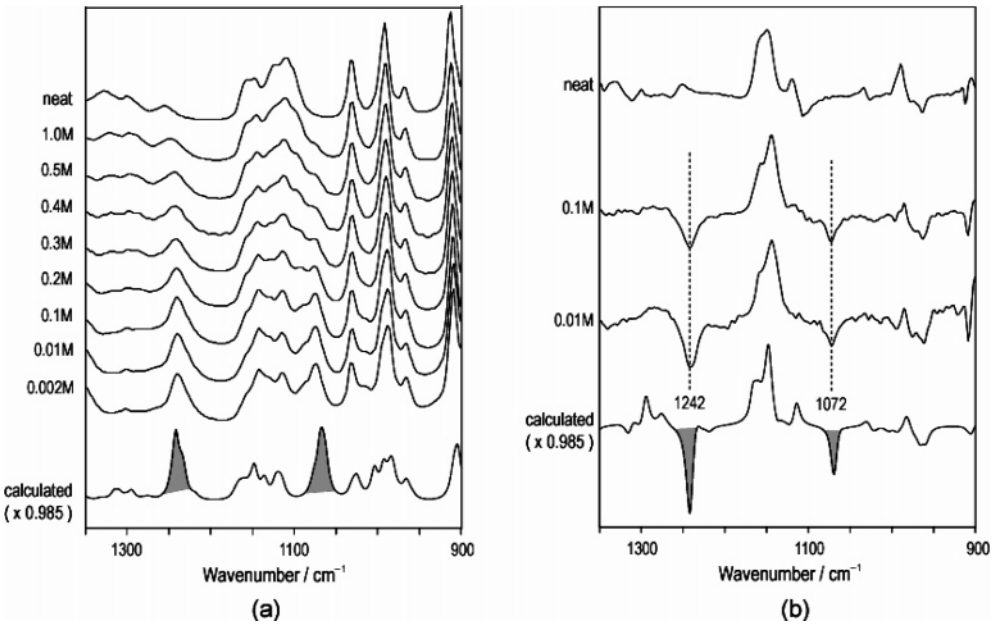

Figure 3. (a) IR and (b) VCD spectra of (*S*)-(+)-2-butanol at various concentrations. CS_2 was used as a solvent. Bottom traces are calculated spectra, scaled by 0.985.

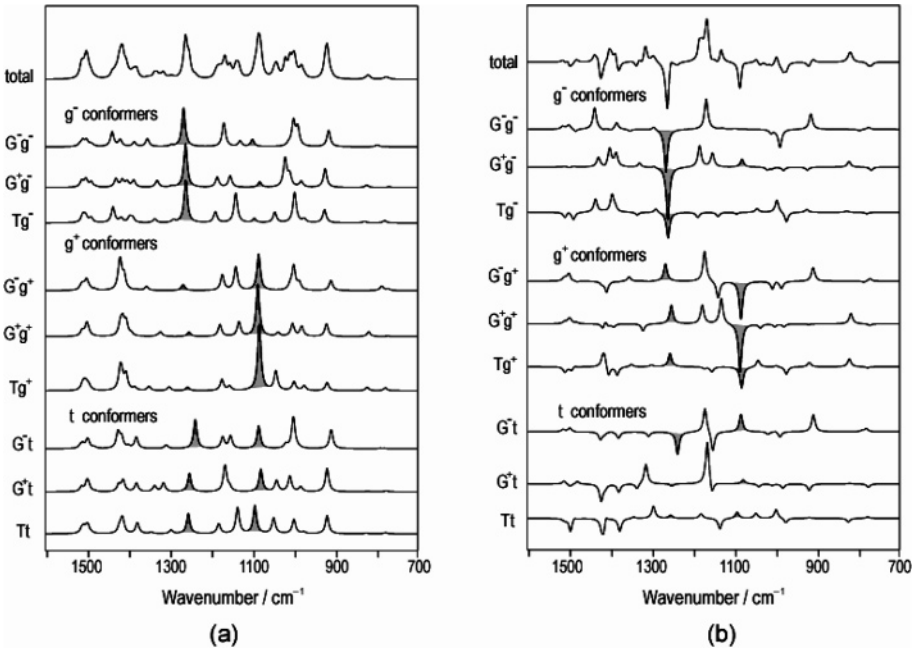

Figure 4. Calculated spectra for the isomers of (*S*)-(+)-2-butanol at the B3LYP/6-31++G(d,p) level: (a) IR, (b) VCD. Shaded peaks correspond to the OH bending mode.

TABLE 1: Gibbs Free Energy Difference (ΔG) and Populations of (*S*)-(+)-2-Butanol Conformers[a]

	ΔG^b (kJ/mol)	relative population (%)
G^+t	0.0	24.9
G^+g^-	0.3	22.0
G^+g^+	1.0	16.3
Tg^-	2.1	10.8
Tt	2.2	10.1
Tg^+	3.0	7.5
G^-g^-	5.1	3.3
G^-t	5.1	3.2
G^-g^+	6.6	1.8

[a] Obtained from B3LYP/6-31++G(d,p) calculations. [b] Difference from G^+t.

TABLE 2: Classification of the OH Bending Bands of (*S*)-(+)-2-Butanol

	band I		band II	
	IR	VCD	IR	VCD
g^-	strong	negative, strong	weak	almost inactive
g^+	weak	positive, medium	strong	negative, strong
t	medium	almost inactive	medium	positive, weak

The main characteristics, summarized in Table 2, seem to depend on the conformation of the OH group.

4. Normal-Mode Analyses and Assignments

The normal vibrational modes of 2-butanol are investigated in detail to explain the above-mentioned features in relation to the molecular vibrations. The normal-mode analyses are carried out with the local symmetry coordinates defined in a standard way.[22,23] Definitions of the local symmetry coordinates are listed in Table 3.

According to the results of the PED analyses, band I is assigned mainly to OH bending, CH deformations, C^1H_3 and C^4H_3 rockings, and C^3H_2 deformations. The $C^1H_3-CHOH-$ part of the molecule is deformed mainly in the g^- and G^-g^+ conformers, whereas the $C^4H_3-C^3H_2-CHOH-$ part is deformed in the t and other g^+ conformers.

TABLE 3: Definitions of Local Symmetry Coordinates[a]

S_1: C^1H_3 s-str.	S_{15}: C^1H_3 s-def.	S_{30}: C^4H_3 s-def.
S_2: C^1H_3 d′-str.	S_{16}: C^1H_3 d′-def.	S_{31}: C^4H_3 d′-def.
S_3: C^1H_3 d″-str.	S_{17}: C^1H_3 d″-def.	S_{32}: C^4H_3 d″-def.
S_4: CH str.	S_{18}: C^1H_3 d′-rock.	S_{33}: C^4H_3 d′-rock
S_5: C^3H_2 s-str.	S_{19}: C^1H_3 d″-rock.	S_{34}: C^4H_3 d″-rock.
S_6: C^3H_2 a-str.	S_{20}: CH def.	S_{35}: OH bend.
S_7: C^4H_3 s-str.	S_{21}: CH def.	S_{36}: C^1C^2 tor.
S_8: C^4H_3 d′-str.	S_{22}: $C^2C^1C^3O$ def.	S_{37}: C^2C^3 tor.
S_9: C^4H_3 d″-str.	S_{23}: $C^2C^1C^3O$ def.	S_{38}: C^3C^4 tor.
S_{10}: OH str.	S_{24}: $C^2C^1C^3O$ def.	S_{39}: CO tor.
S_{11}: C^1C^2 str.	S_{25}: C^3H_2 rock.	
S_{12}: C^2C^3 str.	S_{26}: C^3H_2 wag.	
S_{13}: C^3C^4 str.	S_{27}: C^3H_2 twist.	
S_{14}: CO str.	S_{28}: C^3H_2 sci.	
	S_{29}: $C^2C^3C^4$ bend.	

[a] Combinations of the internal coordinates follow standard definitions.[22,23]

Band II is assigned mainly to OH bending, skeletal stretchings, and C^1H_3 and C^4H_3 rockings. This band of the g^+ conformers has a large contribution from the CO stretching mode, whereas that of other conformers have larger contribution from CC stretchings rather than CO stretching. No other specific features related to the conformers can be found about band II.

5. Rotational Strengths in Local Symmetry Coordinates

The rotational strengths are described in terms of the local symmetry coordinates to investigate the relations between the VCD spectra and the above-mentioned features of the vibrational modes.

The vibrational rotational strength of the *k*th normal mode is expressed as

$$R_k = \frac{\hbar}{2}\left(\frac{\partial \boldsymbol{\mu}}{\partial Q_k}\right)\cdot\left(\frac{\partial \boldsymbol{m}}{\partial P_k}\right) \qquad (1)$$

where $\boldsymbol{\mu}$ and $\boldsymbol{m}$ are the electric and magnetic dipole moment vectors, respectively, Q_k is the normal coordinate of mode *k*, and P_k is the conjugate momentum of Q_k. It is convenient to

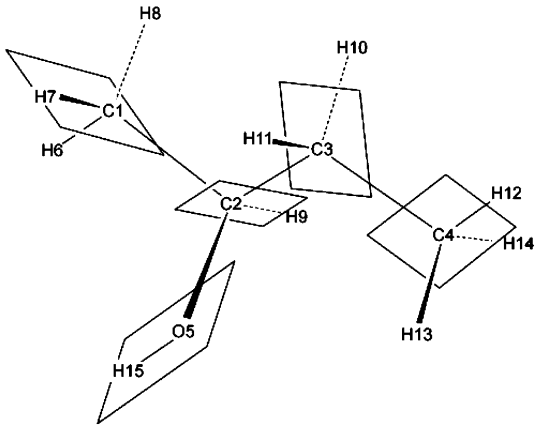

Figure 5. Local symmetry planes defined for band I of the G+t conformer.

use the local symmetry coordinates in the analysis of molecular vibrations. The normal coordinate, $\boldsymbol{Q}$, is a linear combination of the local symmetry coordinate, $\boldsymbol{S}$, and $\boldsymbol{S}$ is represented in a matrix form as

$$\boldsymbol{S} = L_s \boldsymbol{Q} \tag{2}$$

where L_s is the transformation matrix,[22,23] and then

$$\frac{\partial \boldsymbol{\mu}}{\partial Q_k} = \sum_i \frac{\partial \boldsymbol{\mu}}{\partial S_i}\frac{\partial S_i}{\partial Q_k} = \sum_i \frac{\partial \boldsymbol{\mu}}{\partial S_i} L_{s_{i,k}} \tag{3}$$

$$\frac{\partial \boldsymbol{m}}{\partial P_k} = \sum_j \frac{\partial \boldsymbol{m}}{\partial \dot{S}_j}\frac{\partial \dot{S}_j}{\partial P_k} = \sum_j \frac{\partial \boldsymbol{m}}{\partial \dot{S}_j} L_{s_{j,k}} \tag{4}$$

Substituting eqs 3 and 4 into eq 1, we obtain the rotational strength of the *k*th normal mode

$$R_k = \frac{\hbar}{2}\sum_i \sum_j \left(\frac{\partial \boldsymbol{\mu}}{\partial S_i} L_{s_{i,k}}\right)\cdot\left(\frac{\partial \boldsymbol{m}}{\partial \dot{S}_j} L_{s_{j,k}}\right) \tag{5}$$

Now we define

$$R_k^{ij} = \frac{\hbar}{2}\left(\frac{\partial \boldsymbol{\mu}}{\partial S_i} L_{s_{i,k}}\right)\cdot\left(\frac{\partial \boldsymbol{m}}{\partial \dot{S}_j} L_{s_{j,k}}\right) \tag{6}$$

$$R_k(S_i, S_j) = R_k^{ij} + R_k^{ji} - \delta_{ji} R_k^{ji} \tag{7}$$

where δ_{ji} is Kronecker's delta. In eq 7, $R_k(S_i, S_j)$ expresses the contribution of the coupling of S_i and S_j to the rotational strength of the *k*th normal mode. The $R_k(S_i, S_j)$ values are origin-independent (see Appendix), although $\partial \boldsymbol{m}/\partial \dot{S}_i$ and $\partial \boldsymbol{m}/\partial \dot{S}_j$ are origin-dependent.

6. Rotational Strengths Distributed to the Local Modes of (*S*)-(+)-2-Butanol

The $R_k(S_i, S_j)$ values of bands I and II of each conformer of (*S*)-(+)-2-butanol have been calculated, and those with absolute values exceeding 5.0 are listed in Table 4. Some of the major PED values are also listed. The local symmetry planes are defined for individual conformers, as exemplified in Figure 5, to provide the best separations of PEDs. The $R_k(S_i, S_j)$ value of bands I and II are denoted as $R_{\mathrm{I}}(S_i, S_j)$ and $R_{\mathrm{II}}(S_i, S_j)$, respectively.

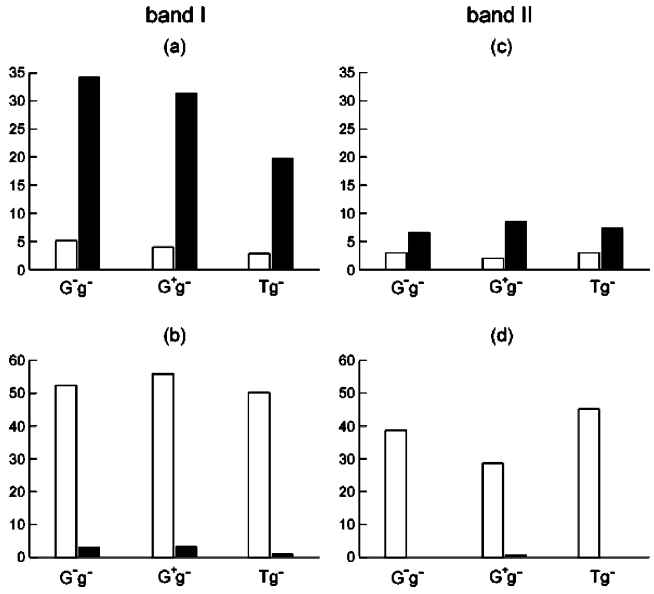

Figure 6. Sums of the absolute values of $R_k(S_i, S_j)$ and PEDs related to the C^1H_3 and OH deformation modes of the g⁻ conformers. The local symmetry plane is defined in Figure 8a. The symbols denote as follows. (a) Sum of the absolute values of $R_k(S_i, S_j)$ of □: symmetric−symmetric or antisymmetric−antisymmetric and ■: symmetric−antisymmetric couplings of band I. (b) Sum of the PED values of □: symmetric and ■: antisymmetric modes of band I, (c) Sum of the absolute values of $R_k(S_i, S_j)$ of □: symmetric−symmetric or antisymmetric−antisymmetric and ■: symmetric−antisymmetric couplings of band II, (d) Sum of the PED values of □: symmetric and ■: antisymmetric modes of band II.

The rotational strengths of band I of the g⁻ conformers are assigned mainly to $R_{\mathrm{I}}(S_{19}, S_{35})$, $R_{\mathrm{I}}(S_{27}, S_{35})$, $R_{\mathrm{I}}(S_{19}, S_{20})$, and $R_{\mathrm{I}}(S_{25}, S_{35})$. These are consistent with the results of the PED analyses. As for band II of the g⁻ conformers, it is assigned mainly to $R_{\mathrm{II}}(S_{33}, S_{35})$, $R_{\mathrm{II}}(S_{25}, S_{35})$, and $R_{\mathrm{II}}(S_{19}, S_{35})$. The CC stretching modes (S_{11}, S_{12}, S_{13}), which have large PED values, scarcely contribute to the rotational strengths. One of the reasons for this may be the small charge redistributions caused by these modes.

Judging from the above-mentioned analyses of bands I and II of the g⁻ conformers, the couplings between OH bending (S_{35}) and CH_3 rockings (S_{18}, S_{19}; S_{33}, S_{34}) appear to have substantial effects on the rotational strengths. However, the contributuions of the OH bending (S_{35}) and C^1H_3 rocking (S_{18}, S_{19}) coupling to the rotational strength of band II are much smaller than those to the rotational strength of band I. This can be explained as follows: Figure 6 shows the sums of the absolute values of $R_k(S_i, S_j)$ and PEDs related to the C^1H_3 and OH deformation modes of the g⁻ conformers with the local symmetry plane including the C^1H^8 bond, as defined in Figure 8a. A part of the numerical data are shown in Table 5, and the detailed ones are deposited in Supporting Information Table S1. The symmetric (S_{14}, S_{18}, S_{35}) and antisymmetric (S_{19}, S_{39}) modes have nonzero PED values in band I of the g⁻ conformers (see Figure 8a). The couplings between these locally symmetric and antisymmetric modes, such as S_{35} and S_{19}, S_{18} and S_{39}, and S_{35} and S_{39}, contribute largely to the rotational strengths. This is consistent with the symmetric characters of $\partial \boldsymbol{\mu}/\partial S_i$ and $\partial m/\partial \dot{S}_j$ under the C_s point group. Band II of the g⁻ conformers, however, has major PED values of C^1H_3 d′-deformation (S_{18}) but has only a negligible contribution from C^1H_3 d″-deformation (S_{19}). This causes small $R_{\mathrm{II}}(S_{18}, S_{35})$ and $R_{\mathrm{II}}(S_{19}, S_{35})$ values because both S_{18} and S_{35} are symmetric.

TABLE 4: Major $R_k(S_i, S_j)$ and PED Values for Bands I and II[a]

band I			band II		
G^-g^- (-35.3)[b]	G^+g^- (-43.7)[b]	Tg^- (-21.5)[b]	G^-g^- (0.7)[b]	G^+g^- (7.5)[b]	Tg^- (-1.7)[b]
$R_I(S_{19}, S_{35}) = -17.9$ $R_I(S_{27}, S_{35}) = -9.1$ $R_I(S_{23}, S_{35}) = 7.0$ $R_I(S_{34}, S_{35}) = -6.3$ $R_I(S_{19}, S_{39}) = 6.3$	$R_I(S_{19}, S_{35}) = -17.7$ $R_I(S_{19}, S_{20}) = -7.2$ $R_I(S_{33}, S_{35}) = -6.5$ $R_I(S_{19}, S_{39}) = 5.8$ $R_I(S_{27}, S_{35}) = -5.3$ $R_I(S_{23}, S_{35}) = 5.2$ $R_I(S_{17}, S_{35}) = -5.2$	$R_I(S_{27}, S_{35}) = -20.6$ $R_I(S_{19}, S_{35}) = -11.3$ $R_I(S_{25}, S_{35}) = 10.8$ $R_I(S_{35}, S_{37}) = 7.9$ $R_I(S_{35}, S_{38}) = 6.6$ $R_I(S_{19}, S_{20}) = -5.8$	$R_{II}(S_{33}, S_{35}) = 10.6$	$R_{II}(S_{19}, S_{35}) = 6.9$ $R_{II}(S_{33}, S_{35}) = 5.9$	$R_{II}(S_{25}, S_{35}) = -9.0$
PED			PED		
S_{35}: 42.1 S_{20}: 12.2 S_{27}: 10.0 S_{19}: 9.6	S_{35}: 47.1 S_{20}: 18.8 S_{19}: 9.8	S_{35}: 42.8 S_{20}: 14.5 S_{27}: 12.4	S_{35}: 28.6 S_{12}: 16.8 S_{11}: 9.2	S_{13}: 24.2 S_{35}: 17.7 S_{33}: 11.4 S_{12}: 10.7	S_{35}: 26.7 S_{12}: 14.7 S_{18}: 12.9 S_{34}: 10.6
G^-g^+ (14.3)[b]	G^+g^+ (15.5)[b]	Tg^+ (11.4)[b]	G^-g^+ (-36.7)[b]	G^+g^+ (-46.6)[b]	Tg^+ (-20.6)[b]
$R_I(S_{19}, S_{35}) = 15.3$ $R_I(S_{24}, S_{35}) = 10.1$ $R_I(S_{22}, S_{35}) = -7.4$	$R_I(S_{27}, S_{35}) = 11.5$ $R_I(S_{34}, S_{35}) = 6.5$ $R_I(S_{19}, S_{35}) = 6.3$	$R_I(S_{25}, S_{35}) = -19.0$ $R_I(S_{27}, S_{35}) = 16.4$ $R_I(S_{33}, S_{35}) = 7.9$ $R_I(S_{19}, S_{35}) = 6.6$ $R_I(S_{22}, S_{25}) = 6.6$ $R_I(S_{35}, S_{37}) = -5.9$ $R_I(S_{22}, S_{27}) = -5.5$	$R_{II}(S_{14}, S_{33}) = -12.7$ $R_{II}(S_{18}, S_{35}) = -12.5$ $R_{II}(S_{33}, S_{35}) = -12.4$ $R_{II}(S_{14}, S_{18}) = -8.0$ $R_{II}(S_{18}, S_{22}) = -5.3$ $R_{II}(S_{22}, S_{33}) = -5.2$ $R_{II}(S_{14}, S_{22}) = 5.1$	$R_{II}(S_{33}, S_{35}) = -12.1$ $R_{II}(S_{19}, S_{35}) = -10.3$ $R_{II}(S_{14}, S_{19}) = -7.1$ $R_{II}(S_{14}, S_{33}) = -6.5$ $R_{II}(S_{27}, S_{35}) = 5.6$ $R_{II}(S_{24}, S_{35}) = -5.4$	$R_{II}(S_{19}, S_{35}) = -9.4$ $R_{II}(S_{25}, S_{35}) = 8.6$ $R_{II}(S_{14}, S_{19}) = -7.5$ $R_{II}(S_{34}, S_{35}) = -6.0$ $R_{II}(S_{27}, S_{35}) = 5.8$
PED			PED		
S_{35}: 37.5 S_{20}: 17.2 S_{19}: 10.7	S_{35}: 21.3 S_{27}: 18.1 S_{34}: 17.3 S_{25}: 11.6 S_{20}: 10.0	S_{35}: 25.9 S_{21}: 14.6 S_{33}: 14.2 S_{27}: 13.4	S_{35}: 28.0 S_{33}: 24.0 S_{18}: 12.4 S_{14}: 10.0	S_{35}: 36.7 S_{19}: 15.7 S_{14}: 12.4	S_{35}: 34.7 S_{14}: 17.7 S_{19}: 16.2 S_{34}: 13.0
G^-t (-19.2)[b]	G^+t (-2.0)[b]	Tt (2.5)[b]	G^-t (16.9)[b]	G^+t (4.0)[b]	Tt (6.0)[b]
$R_I(S_{25}, S_{35}) = -9.3$ $R_I(S_{20}, S_{25}) = 6.3$ $R_I(S_{35}, S_{36}) = -6.0$	$R_I(S_{25}, S_{35}) = 13.5$ $R_I(S_{34}, S_{35}) = -11.6$ $R_I(S_{20}, S_{35}) = 10.3$ $R_I(S_{20}, S_{25}) = 9.1$ $R_I(S_{25}, S_{39}) = -7.6$ $R_I(S_{20}, S_{34}) = -6.1$ $R_I(S_{27}, S_{35}) = -5.5$	$R_I(S_{25}, S_{35}) = 16.1$ $R_I(S_{27}, S_{35}) = -12.6$ $R_I(S_{33}, S_{35}) = -8.6$ $R_I(S_{20}, S_{35}) = 7.8$ $R_I(S_{35}, S_{37}) = 6.1$	$R_{II}(S_{18}, S_{35}) = 9.4$ $R_{II}(S_{34}, S_{35}) = 6.3$	$R_{II}(S_{24}, S_{35}) = 8.4$ $R_{II}(S_{25}, S_{35}) = -6.0$ $R_{II}(S_{12}, S_{35}) = -5.5$	$R_{II}(S_{19}, S_{35}) = 5.4$
PED			PED		
S_{35}: 42.6 S_{20}: 22.7 S_{33}: 7.8	S_{35}: 28.7 S_{20}: 21.5 S_{34}: 13.5	S_{20}: 30.0 S_{35}: 28.8 S_{33}: 10.8	S_{35}: 27.3 S_{13}: 23.1 S_{12}: 15.1 S_{18}: 10.1	S_{35}: 30.0 S_{11}: 16.0 S_{12}: 14.8	S_{35}: 33.3 S_{12}: 22.6 S_{11}: 11.9

[a] $R_k(S_i, S_j)$ values with absolute values exceeding 5.0 are listed. $R_k(S_i, S_j)$ values are in units of 10^{-44} esu^2 cm^2. The local symmetry planes are defined for individual conformers to provide the best separations of PEDs of symmetric and antisymmetric modes. Note that $R_k(S_i, S_j)$ and $R_k(S_j, S_i)$ are identical. [b] Numbers in parentheses represent the rotational strengths in units of 10^{-44} esu^2 cm^2.

The rotational strengths of band I of the t conformers are assigned mainly to $R_I(S_{25}, S_{35})$, $R_I(S_{27}, S_{35})$, $R_I(S_{34}, S_{35})$, $R_I(S_{20}, S_{35})$, and so forth, as shown in Table 4. These are consistent with the results of the PED analyses as a whole. However, the $R_k(S_i, S_j)$ values of band II for the t conformers are, in general, small, and only the couplings between OH bending (S_{35}) and CH_3 rocking (S_{18}, S_{19}; S_{33}, S_{34}) and between OH bending and $C^2C^1C^3O$ deformation (S_{24}) have major values. The CC stretching modes (S_{11}, S_{12}, S_{13}), which have large PED values, hardly contribute to the rotational strengths, as is the case with the g^- conformers.

The discussion about the locally symmetric and antisymmetric mode couplings made for the g^- conformers is also applicable for the Tt conformer. Figure 7 shows the sums of the absolute values of $R_k(S_i, S_j)$ and PEDs related to the C^4H_3, C^3H_2, and OH group deformation modes of the Tt conformer with the local symmetry plane including the C^4H^{12} bond as defined in Figure 8b. Detailed numerical data are deposited in Supporting Information Table S2. Band I of the Tt conformer is assigned to both the symmetric and antisymmetric modes (see Figure 8b), whereas band II is assigned almost entirely to the symmetric modes. This gives rise to the large $R_I(S_i, S_j)$ values of locally symmetric and antisymmetric mode couplings, such as $R_I(S_{35}, S_{25})$, $R_I(S_{35}, S_{27})$, $R_I(S_{35}, S_{34})$, and small $R_{II}(S_i, S_j)$ values.

The general features of the g^- and t conformers are such that band I is contributed from locally symmetric and antisymmetric modes, whereas band II is contributed almost exclusively from symmetric modes. As a result, band I of the g^- and t conformers may have large $R_k(S_i, S_j)$ values, whereas band II of these conformers must have small $R_k(S_i, S_j)$ values. The weak VCD intensities of band I of the t conformers are caused by cancellation of the $R_I(S_i, S_j)$ values.

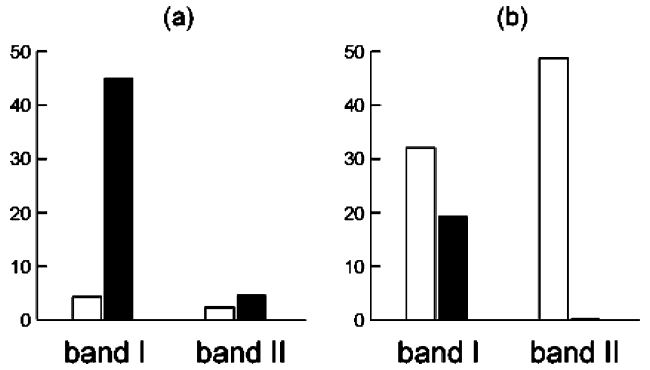

Figure 7. Sums of the absolute values of $R_k(S_i, S_j)$ and PEDs related to the C^4H_3, C^3H_2 and OH group deformation modes of the Tt conformer. The local symmetry plane is defined in Figure 8b. The symbols denote as follows. (a) Sum of the absolute values of $R_k(S_i, S_j)$ of □: symmetric−symmetric or antisymmetric−antisymmetric and ■: symmetric−antisymmetric couplings. (b) Sum of the PED values of □: symmetric and ■: antisymmetric modes.

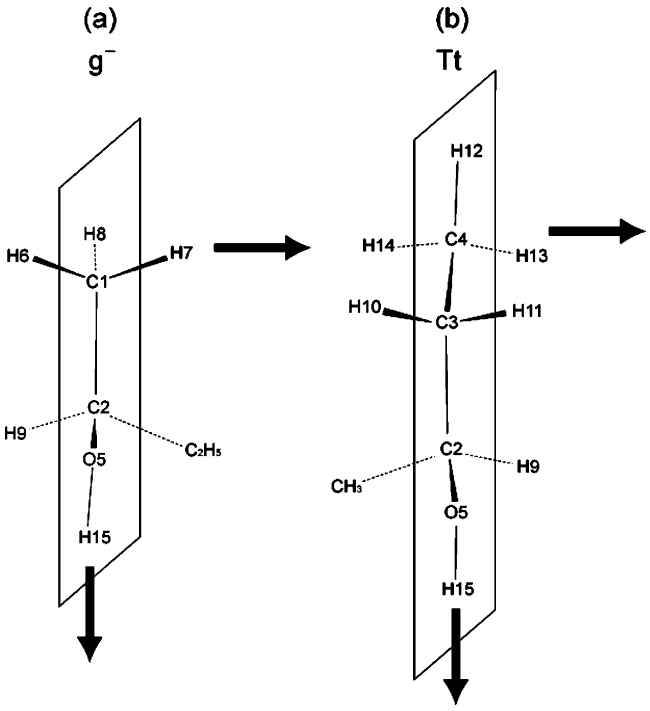

Figure 8. Locally symmetric and antisymmetric mode couplings of (a) g^- conformers and (b) Tt conformer.

The rotational strengths of bands I and II of the g^+ conformers have large contributions from the couplings between OH bending (S_{35}) and other local modes, such as C^1H_3 rockings (S_{18}, S_{19}), C^4H_3 rockings (S_{33}, S_{34}), and CH_2 rocking (S_{25}) and twisting (S_{27}), as shown in Table 4. The contribution of CO stretching (S_{14}) and CH_3 rocking (S_{18}, S_{19}; S_{33}, S_{34}) coupling is unique to band II of the g^+ conformers, and this is consistent with the results of the PED analyses. Unlike the g^- and t conformers, the rotational strengths of bands I and II of the g^+ conformers are hardly interpretable by the local symmetry. The C^1C^2 and C^2C^3 bonds are out of the C^2OH plane, and the combinations of such as OH bending and CH_3 rockings, and CO stretching and CH_3 rockings deviate further from orthogonality about their vibrational displacements. Both bands I and II of the g^+ conformers can thus have large $R_k(S_i, S_j)$ values, and the small VCD intensities of band I are due to the cancellations among the $R_I(S_i, S_j)$ values.

TABLE 5: $R_k(S_i, S_j)$ and PED Values of Band I Related to the C^1H_3 and OH Group Deformation Modes of the G^-g^- Conformer[a]

band I (−35.3)[b]	
$R_k(S_i, S_j)$	PED
$R_I(S_{18}, S_{35}) = -2.7$	S_{14}: 3.6
$R_I(S_{18}, S_{14}) = -1.2$	S_{18}: 6.7
$R_I(S_{35}, S_{14}) = 1.0$	S_{35}: 42.1
$R_I(S_{19}, S_{39}) = 0.2$	
$R_I(S_{35}, S_{19}) = -16.3$	S_{19}: 3.0
$R_I(S_{18}, S_{39}) = 5.9$	S_{39}: 0.1
$R_I(S_{14}, S_{19}) = -4.0$	
$R_I(S_{14}, S_{39}) = 3.4$	
$R_I(S_{35}, S_{39}) = -4.6$	

[a] $R_k(S_i, S_j)$ values are in units of 10^{-44} esu^2 cm^2. The local symmetry plane is defined in Figure 8a. The horizontal line separates the $R_k(S_i, S_j)$ entries into the symmetric−symmetric or antisymmetric−antisymmetric couplings (upper) and symmetric−antisymmetric couplings (lower), and the PED entires into symmetric (upper) and antisymmetric (lower) modes. $R_k(S_i, S_j)$ and $R_k(S_j, S_i)$ are identical. [b] The number in parentheses represents the rotational strength in units of 10^{-44} esu^2 cm^2.

In summary of the foregoing discussions, the coupling of CH_3 rocking and OH bending modes commonly plays a significant role in the rotational strengths of bands I and II of the g^-, g^+, and t conformers. The local symmetry of the CH_3 group vibrations is broken easily by an asymmetric structural environment. This eventually results in the locally symmetric and antisymmetric couplings between the CH_3 and other groups.

The contributions of CH_2 rockings (S_{25}) and twistings (S_{27}) are also notable. The couplings between CH_2 rocking or twisting and other local vibrational modes often have large $R_k(S_i, S_j)$ values. The large contribution of the CH_2 rocking mode to VCD was also emphasized by Nafie, Freedman et al.[24,25] They reported that the local circulatory electron current density about the centers of carbon and oxygen atoms had been observed for the CH_2 rocking and some other modes of formaldehyde and ethylene. They described that these circulatory motions of electron current density contribute to giving rise to magnetic dipole moments. Our way of presentation of the local mode contribution to the VCD activity is independent of their scheme. However, there must be some connection between these two schemes, because both have clarified the essential role of the CH_2 rocking mode in different molecules. A more comprehensive investigation of the coherent physical meanings contained in the above-mentioned two schemes may reveal the origins of $\partial\boldsymbol{\mu}/\partial S_i$ and $\partial\boldsymbol{m}/\partial\dot{S}_j$, and thereby the detailed mechanism of VCD.

7. Conclusions

The rotational strengths of the two OH bending bands of (*S*)-(+)-2-butanol are contributed mainly from the couplings of OH bending with CH_3 rockings and CH_2 rocking and twisting. The characteristic features can be explained by the direction of displacement of each local group. Bands I of the g^- and t conformers have contributions from locally symmetric and antisymmetric vibrational modes, which provide significant $R_k(S_i, S_j)$ values. Small VCD intensities of the t conformers arise from cancellations of $R_k(S_i, S_j)$ values with opposite signs. Bands II of the g^- and t conformers are assigned almost exclusively to the symmetric modes, which lead to small $R_k(S_i, S_j)$ values, and hence, small VCD intensities. However, the rotational strengths of bands I and II of the g^+ conformers are hardly explicable by local symmetry; these bands are likely to have

large $R_k(S_i, S_j)$ values, although cancellations of $R_k(S_i, S_j)$ values with opposite signs cause the small VCD intensities of band I.

In summary, the couplings of locally symmetric and antisymmetric modes play essential roles in producing large rotational strengths. A further study along this line will afford novel insight into the relationship between VCD and molecular vibrations.

Acknowledgment. We are grateful to Professor Kozo Kuchitsu for his helpful comments on the manuscript. We thank the University of the Air for the special grant.

Supporting Information Available: Detailed numerical data. This material is available free of charge via the Internet at http://pubs.acs.org.

Appendix

The origin independence of $R_k(S_i, S_j)$ is proved as follows. Assume that we move the origin from **O** to **W**. Then the following relations are obtained[5]

$$\left(\frac{\partial \mu_\alpha}{\partial X_{A\chi}}\right)^{\mathbf{W}} = \left(\frac{\partial \mu_\alpha}{\partial X_{A\chi}}\right)^{\mathbf{O}} \tag{A1}$$

$$\left(\frac{\partial m_\alpha}{\partial \dot{X}_{A\chi}}\right)^{\mathbf{W}} = \left(\frac{\partial m_\alpha}{\partial \dot{X}_{A\chi}}\right)^{\mathbf{O}} - \frac{1}{2}\in_{\alpha\beta\gamma} Y_\beta \frac{\partial \mu_\gamma}{\partial X_{A\chi}} \tag{A2}$$

where $\boldsymbol{X}_A$ is the Cartesian coordinate of atom A, α, β, γ, and χ are the Cartesian coordinate elements, $\boldsymbol{Y}$ is the vector from **O** to **W**, and $\in_{\alpha\beta\gamma}$ is the alternating tensor. Using these equations, we obtain the following relations:

$$\begin{aligned}\left(\frac{\partial \mu_\alpha}{\partial S_i}\right)^{\mathbf{W}} &= \sum_A \sum_\chi \left(\frac{\partial \mu_\alpha}{\partial X_{A\chi}}\right)^{\mathbf{W}} \frac{\partial X_{A\chi}}{\partial S_i} \\ &= \sum_A \sum_\chi \left(\frac{\partial \mu_\alpha}{\partial X_{A\chi}}\right)^{\mathbf{O}} \frac{\partial X_{A\chi}}{\partial S_i} \\ &= \left(\frac{\partial \mu_\alpha}{\partial S_i}\right)^{\mathbf{O}}\end{aligned} \tag{A3}$$

$$\begin{aligned}\left(\frac{\partial m_\alpha}{\partial \dot{S}_j}\right)^{\mathbf{W}} &= \sum_A \sum_\chi \left(\frac{\partial m_\alpha}{\partial \dot{X}_{A\chi}}\right)^{\mathbf{W}} \frac{\partial \dot{X}_{A\chi}}{\partial \dot{S}_j} \\ &= \sum_A \sum_\chi \left(\left(\frac{\partial m_\alpha}{\partial \dot{X}_{A\chi}}\right)^{\mathbf{O}} - \frac{1}{2}\in_{\alpha\beta\gamma} Y_\beta \frac{\partial \mu_\gamma}{\partial X_{A\chi}}\right) \frac{\partial \dot{X}_{A\chi}}{\partial \dot{S}_j} \\ &= \left(\frac{\partial m_\alpha}{\partial \dot{S}_j}\right)^{\mathbf{O}} - \frac{1}{2}\in_{\alpha\beta\gamma} Y_\beta \frac{\partial \mu_\gamma}{\partial S_j}\end{aligned} \tag{A4}$$

The vector expressions of eqs A3 and A4 are

$$\left(\frac{\partial \boldsymbol{\mu}}{\partial S_i}\right)^{\mathbf{W}} = \left(\frac{\partial \boldsymbol{\mu}}{\partial S_i}\right)^{\mathbf{O}} \tag{A5}$$

and

$$\left(\frac{\partial \boldsymbol{m}}{\partial \dot{S}_j}\right)^{\mathbf{W}} = \left(\frac{\partial \boldsymbol{m}}{\partial \dot{S}_j}\right)^{\mathbf{O}} - \frac{1}{2}\left(\boldsymbol{Y} \times \frac{\partial \boldsymbol{\mu}}{\partial S_j}\right) \tag{A6}$$

respectively. By using eqs A5 and A6, the origin independence of $R_k(S_i, S_j)$ is examined as follows: when $i \neq j$

$$\begin{aligned}R_k(S_i, S_j)^{\mathbf{W}} &= \frac{\hbar}{2}\left(\left(\frac{\partial \boldsymbol{\mu}}{\partial S_i}\right)^{\mathbf{O}} L_{s_{i,k}}\right)\cdot\left\{\left(\frac{\partial \boldsymbol{m}}{\partial \dot{S}_j}\right)^{\mathbf{O}} - \frac{1}{2}\left(\boldsymbol{Y} \times \left(\frac{\partial \boldsymbol{\mu}}{\partial S_j}\right)^{\mathbf{O}}\right)\right\} L_{s_{j,k}} \\ &+ \frac{\hbar}{2}\left(\left(\frac{\partial \boldsymbol{\mu}}{\partial S_j}\right)^{\mathbf{O}} L_{s_{j,k}}\right)\cdot\left\{\left(\frac{\partial \boldsymbol{m}}{\partial \dot{S}_i}\right)^{\mathbf{O}} - \frac{1}{2}\left(\boldsymbol{Y} \times \left(\frac{\partial \boldsymbol{\mu}}{\partial S_i}\right)^{\mathbf{O}}\right)\right\} L_{s_{i,k}} \\ &= \frac{\hbar}{2}\left[\left\{\left(\left(\frac{\partial \boldsymbol{\mu}}{\partial S_i}\right)^{\mathbf{O}} L_{s_{i,k}}\right)\cdot\left(\left(\frac{\partial \boldsymbol{m}}{\partial \dot{S}_j}\right)^{\mathbf{O}} L_{s_{j,k}}\right)\right.\right. \\ &+ \left.\left.\left(\left(\frac{\partial \boldsymbol{\mu}}{\partial S_j}\right)^{\mathbf{O}} L_{s_{j,k}}\right)\cdot\left(\left(\frac{\partial \boldsymbol{m}}{\partial \dot{S}_i}\right)^{\mathbf{O}} L_{s_{i,k}}\right)\right\}\right. \\ &- \frac{1}{2} L_{s_{i,k}} L_{s_{j,k}}\left\{\left(\frac{\partial \boldsymbol{\mu}}{\partial S_i}\right)^{\mathbf{O}}\cdot\left(\boldsymbol{Y} \times \left(\frac{\partial \boldsymbol{\mu}}{\partial S_j}\right)^{\mathbf{O}}\right)\right. \\ &+ \left.\left.\left(\frac{\partial \boldsymbol{\mu}}{\partial S_j}\right)^{\mathbf{O}}\cdot\left(\boldsymbol{Y} \times \left(\frac{\partial \boldsymbol{\mu}}{\partial S_i}\right)^{\mathbf{O}}\right)\right\}\right] \\ &= R_k(S_i, S_j)^{\mathbf{O}} - \frac{\hbar}{4} L_{s_{i,k}} L_{s_{j,k}}\left\{\left(\frac{\partial \boldsymbol{\mu}}{\partial S_i}\right)^{\mathbf{O}}\cdot\left(\boldsymbol{Y} \times \left(\frac{\partial \boldsymbol{\mu}}{\partial S_j}\right)^{\mathbf{O}}\right)\right. \\ &+ \left.\left(\frac{\partial \boldsymbol{\mu}}{\partial S_i}\right)^{\mathbf{O}}\cdot\left(\left(\frac{\partial \boldsymbol{\mu}}{\partial S_j}\right)^{\mathbf{O}} \times \boldsymbol{Y}\right)\right\} \\ &= R_k(S_i, S_j)^{\mathbf{O}}\end{aligned} \tag{A7.1}$$

and when $i = j$

$$\begin{aligned}R_k(S_i, S_i)^{\mathbf{W}} &= \frac{\hbar}{2}\left(\left(\frac{\partial \boldsymbol{\mu}}{\partial S_i}\right)^{\mathbf{O}} L_{s_{i,k}}\right)\cdot\left\{\left(\frac{\partial \boldsymbol{m}}{\partial \dot{S}_i}\right)^{\mathbf{O}} - \frac{1}{2}\left(\boldsymbol{Y} \times \left(\frac{\partial \boldsymbol{\mu}}{\partial S_i}\right)^{\mathbf{O}}\right)\right\} L_{s_{i,k}} \\ &= \frac{\hbar}{2}\left(\left(\frac{\partial \boldsymbol{\mu}}{\partial S_i}\right)^{\mathbf{O}} L_{s_{i,k}}\right)\cdot\left(\left(\frac{\partial \boldsymbol{m}}{\partial \dot{S}_i}\right)^{\mathbf{O}} L_{s_{i,k}}\right) \\ &- \frac{\hbar}{4} L_{s_{i,k}} L_{s_{i,k}}\left(\frac{\partial \boldsymbol{\mu}}{\partial S_i}\right)^{\mathbf{O}}\cdot\left(\boldsymbol{Y} \times \left(\frac{\partial \boldsymbol{\mu}}{\partial S_i}\right)^{\mathbf{O}}\right) \\ &= R_k(S_i, S_i)^{\mathbf{O}} - \frac{\hbar}{4} L_{s_{i,k}} L_{s_{i,k}} \boldsymbol{Y}\cdot\left(\left(\frac{\partial \boldsymbol{\mu}}{\partial S_i}\right)^{\mathbf{O}} \times \left(\frac{\partial \boldsymbol{\mu}}{\partial S_i}\right)^{\mathbf{O}}\right) \\ &= R_k(S_i, S_i)^{\mathbf{O}}\end{aligned} \tag{A7.2}$$

In eqs A7.1 and A7.2, the relation of scalar triple multiplication, $\boldsymbol{A}\cdot(\boldsymbol{B} \times \boldsymbol{C}) = \boldsymbol{B}\cdot(\boldsymbol{C} \times \boldsymbol{A}) = \boldsymbol{C}\cdot(\boldsymbol{A} \times \boldsymbol{B})$, is used. Equations A7.1 and A7.2 show the origin independence of $R_k(S_i, S_j)$.

References and Notes

(1) Stephens, P. J.; Lowe, M. A. *Annu. Rev. Phys. Chem.* **1985**, *36*, 213−241.
(2) Barron, L. D. *Molecular Light Scattering and Optical Activity*; Cambridge University Press: London, 1982.
(3) Polavarapu, P. L. *Vibrational Spectra: Principles and Applications with Emphasis on Optical Activity*; Elsevier: New York, 1998.
(4) Stephens, P. J.; Jalkanen, K. J.; Kawiecki, R. W. *J. Am. Chem. Soc.* **1990**, *112*, 6518−6529.
(5) Stephens, P. J. *J. Phys. Chem.* **1985**, *89*, 748−752.
(6) Stephens, P. J. *J. Phys. Chem.* **1987**, *91*, 1712−1715.
(7) Buckingham, A. D.; Fowler, P. W.; Galwas, P. A. *Chem. Phys.* **1987**, *112*, 1−14.
(8) Nafie, L. A.; Walnut, T. H. *Chem. Phys. Lett.* **1977**, *49*, 441−446.
(9) Walnut, T. H.; Nafie, L. A. *J. Chem. Phys.* **1977**, *67*, 1501−1510.
(10) Nafie, L. A.; Polavarapu, P. L. *J. Chem. Phys.* **1981**, *75*, 2935−2944.
(11) Nafie, L. A.; Freedman, T. B. *J. Chem. Phys.* **1983**, *78*, 7108−7116.
(12) Cheeseman, J. R.; Frisch, M. J.; Devlin, F. J.; Stephens, P. J. *Chem. Phys. Lett.* **1996**, *252*, 211−220.
(13) Bak, K. L.; Jørgensen, P.; Helgaker, T.; Ruud, K.; Jensen, H. J. A. *J. Chem. Phys.* **1993**, *98*, 8873−8887.
(14) London, F. *J. Phys. Radium* **1937**, *10*, 397−409.
(15) Morino, Y.; Kuchitsu, K. *J. Chem. Phys.* **1952**, *20*, 1809−1810.
(16) Wilson, E. B. *J. Chem. Phys.* **1939**, *7*, 1047−1052.
(17) Wilson, E. B. *J. Chem. Phys.* **1941**, *9*, 76−84.

(18) Wilson, E. B.; Decius, J. C.; Cross, P. C. *Molecular Vibrations: The Theory of Infrared and Raman Vibrational Spectra*; McGraw-Hill: New York, 1955.

(19) Frisch, M. J.; Trucks, G. W.; Schlegel, H. B.; Scuseria, G. E.; Robb, M. A.; Cheeseman, J. R.; Zakrzewski, V. G.; Montgomery, J. A., Jr.; Stratmann, R. E.; Burant, J. C.; Dapprich, S.; Millam, J. M.; Daniels, A. D.; Kudin, K. N.; Strain, M. C.; Farkas, O.; Tomasi, J.; Barone, V.; Cossi, M.; Cammi, R.; Mennucci, B.; Pomelli, C.; Adamo, C.; Clifford, S.; Ochterski, J.; Petersson, G. A.; Ayala, P. Y.; Cui, Q.; Morokuma, K.; Malick, D. K.; Rabuck, A. D.; Raghavachari, K.; Foresman, J. B.; Cioslowski, J.; Ortiz, J. V.; Stefanov, B. B.; Liu, G.; Liashenko, A.; Piskorz, P.; Komaromi, I.; Gomperts, R.; Martin, R. L.; Fox, D. J.; Keith, T.; Al-Laham, M. A.; Peng, C. Y.; Nanayakkara, A.; Gonzalez, C.; Challacombe, M.; Gill, P. M. W.; Johnson, B. G.; Chen, W.; Wong, M. W.; Andres, J. L.; Head-Gordon, M.; Replogle, E. S.; Pople, J. A. *Gaussian 98*, revision A.9; Gaussian, Inc.: Pittsburgh, PA, 1998.

(20) Wang, F.; Polavarapu, P. L. *J. Phys. Chem. A* **2000**, *104*, 10683−10687.

(21) Shin, S.; Hamada, Y.; Shinya, K.; Ohno, K. Unpublished data.

(22) Shimanouchi, T. *Nippon Kagaku Zasshi* **1965**, *86*, 261−281.

(23) Shimanouchi, T. *Nippon Kagaku Zasshi* **1965**, *86*, 768−779.

(24) Nafie, L. A. *J. Phys. Chem. A* **1997**, *101*, 7826−7833.

(25) Freedman, T. B.; Shih, M.; Lee, E.; Nafie, L. A. *J. Am. Chem. Soc.* **1997**, *119*, 10620−10626.